Chinese Chemical Letters 31 (2020) 1427–1431

Contents lists available at ScienceDirect

Chinese Chemical Letters

journal homepage: www.elsevier.com/locate/cclet

Communication

Preparation of poly(glutamic acid) shielding micelles self-assembled from polylysine-*b*-polyphenylalanine for gene and drug codelivery

Jing Ma[a,b], Jingpeng Zhang[a,b], Lin Chi[a], Chong Liu[a,b], Yanhui Li[a,*], Huayu Tian[b,*]

[a] School of Materials Science and Engineering, Changchun University of Science and Technology, Changchun 130022, China
[b] Key Laboratory of Polymer Ecomaterials, Changchun Institute of Applied Chemistry, Chinese Academy of Sciences, Changchun 130022, China

ARTICLE INFO

Article history:
Received 27 December 2019
Received in revised form 29 January 2020
Accepted 17 February 2020
Available online 19 February 2020

Keywords:
Codelivery
Shielding
Doxorubicin
Bcl2 siRNA
Cancer therapy

ABSTRACT

A novel amphiphilic cationic block copolymer polylysine-*b*-polyphenylalanine (PLL-*b*-PPhe) was synthesized and self-assembled into micelles in aqueous solution, then shielded with poly(glutamic acid) (marked as PG/PLL-*b*-PPhe) to codeliver gene and drug for combination cancer therapy. Here, doxorubicin (DOX) was selected to be loaded into PLL-*b*-PPhe micelles and the drug loading efficiency was 8.0%. The drug release studies revealed that the PLL-*b*-PPhe micelles were pH sensitive and the released DOX could reach to 53.0%, 65.0%, 72.0% at pH 7.4, 6.8 and 5.0, respectively. In order to reduce positive charge and cytotoxicity of PLL-*b*-PPhe micelles, PG was used as shelding, simultaneously condensed with Bcl2 siRNA to form gene carrier system. Compared with PEI, PG/PLL-*b*-PPhe had excellent gene transfection efficiency, especially when the molar ratio of PLL to PPhe was 30:60 and the mixed mass ratio of PLL-*b*-PPhe to gene was 5:1. More importantly, DOX and Bcl2 siRNA gene codelivery system displayed remarkable cytotoxicity against B16F10 cells. Confocal laser scanning microscopy (CLSM) and flow cytometry were used to characterize endocytosis of the codelivery system, and confirmed that both DOX and Bcl2 siRNA had been endocytosed into B16F10 cells. The above results indicated that gene and drug codelivery was a promising strategy in future cancer therapy.

According to the *Global Cancer Statistics 2018*, there were 1.8 billion new cases of cancer and 9.6 million cancer deaths worldwide in 2018 [1]. Although researchers have taken a lot of efforts for cancer therapy [2–5], the incidence and mortality of cancer are still high. At present, chemotherapy, radiation therapy, surgical resection and gene therapy have used in clinic cancer therapy. Among them, chemotherapy is a common and effective method to kill cancer cells by drugs. However, the traditional anticancer drugs have low bioavailability, short circulation time, high drug toxicity and inefficient tumor penetration [6,7]. So, it is necessary to modify or carry drugs to overcome these disadvantages. Cheng *et al.* used glycol chitosan modified liposomal encapsulated DOX to form a pH-responsive platform, which can effectively kill cancer cells [8]. Zou *et al.* encapsulated doxorubicin in MOF to eliminate breast cancers effectively [9]. Meng *et al.* designed a lipid modified mesoporous silica nanoparticles for co-deliver gemcitabine and paclitaxel to eliminate human pancreatic cancer [10]. However, due to the complexity of the malignant tumors [11], a single chemotherapy cannot inhibit them thoroughly. For example, long-term chemotherapy reduces the sensitivity of cancer cells to anticancer drugs, resulting in multidrug resistance (MDR) [12].

In order to solve this problem, the drug and gene co-delivery system has received extensive attention as a new antitumor strategy [13–18]. The exogenous genes cannot only achieve a certain therapeutic effect but also enhance the effective concentration of chemotherapeutic drugs in cancer cells by silencing the expression of related genes [19–21]. Xu *et al.* investigated the codelivery of DOX and Bcl2 siRNA in polyethyleneimine (PEI) carrier for synergistic anti-tumor therapy [22]. The strategy of codelivery of genes and drugs would acquire therapeutic effects with smaller doses and break a certain limitation of traditional chemotherapy.

The Bcl2 gene is an apoptosis-suppressing gene that inhibits apoptosis of various tissue cells by expressing related proteins [23]. At present, the mechanism of anti-apoptosis of Bcl2 gene mainly includes: (1) antagonizing the pro-apoptotic gene Bax; (2) inhibiting the pro-apoptotic cytochrome C into the cytosol; (3) preventing the cytochrome C activates caspase in the cytoplasm; (4) antioxidation and maintaining intracellular calcium homeostasis [24]. Using RNA interference (RNAi) technology, the introduction of Bcl2 siRNA gene into cancer cells can inhibit the expression of Bcl2 gene and promote the apoptosis of cancer cells [25,26].

* Corresponding authors.
E-mail addresses: lyh2008@cust.edu.cn (Y. Li), thy@ciac.ac.cn (H. Tian).

https://doi.org/10.1016/j.cclet.2020.02.034
1001-8417/

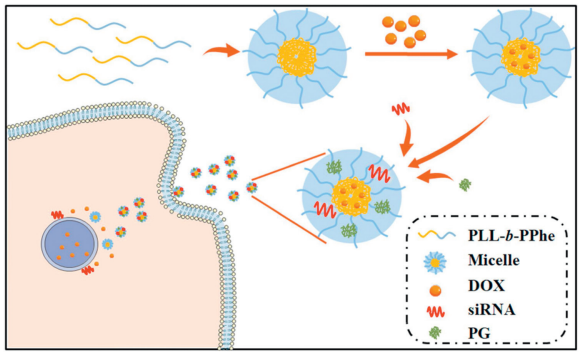

Scheme 1. PG/PLL-*b*-PPhe/DOX/siRNA codelivery nanoparticles for cancer therapy.

Positive polylysine (PLL) has excellent binding ability to negative DNA, which has been used as a gene carrier [27]. However, the high cytotoxicity and the low transfection efficiency limit PLL's application as a polymer gene carrier. In order to improve the transfection efficiency, many attempts had been made to modify PLL, such as introducing polyethylene glycol (PEG) to reduce cytotoxicity, grafting a histidine derivative to increase the lysosomal escape ability of the polycation/pDNA complex, thereby promoting cellular uptake of the complex [28–30].

In this work, polyphenylalanine (PPhe) was selected to graft onto PLL to form block copolymer PLL-*b*-PPhe, then PLL-*b*-PPhe self-assembled into micelles to carry doxorubicin (DOX), last, Bcl2 siRNA gene and a certain amount of polyglutamic acid (PG) compound with the micelles to perform drug and gene codelivery with PG as shielding [31,32] to reduce toxicity by electrostatic interaction. As a result, a novel drug and gene co-delivery system (marked as PG/PLL-*b*-PPhe/DOX/siRNA) was prepared successfully. Finally, B16F10 cells were selected to evaluate the synergistic effect of DOX and Bcl2 siRNA in cancer cell eliminating, and the design was shown in Scheme 1.

The synthesis of the PG and the diblock copolymer PLL-*b*-PPhe was shown in Scheme 2. The PLL-*b*-PPhe was synthesized through three steps. Firstly, PLL(Z) was synthesized by ring-opening polymerization with Lys(Z)-NCA as monomer and *N*-hexylamine as initiator. Secondly, amino-terminated PLL(Z) was used as a macromolecular initiator to induce further ring-opening polymerization with Phe-NCA as monomer. Finally, the amphiphilic diblock copolymers PLL-*b*-PPhe were obtained after the deprotection of PLL(Z)-*b*-PPhe by HBr/HAc in TFA solution. PG, PLL(Z) and three different ratios of PLL-*b*-PPhe (30:20, 30:40, 30:60) were characterized by ^{1}H NMR in Fig. 1. As shown in Fig. 1A, the proton peaks of 4.18 ppm (a, -CH), 2.18 ppm (b, -CH_2) and 1.82 ppm (c, -CH_2) confirmed the successful synthesis of PG. The proton peaks of 7.32-7.01 ppm (d + e+i + j, -C_6H_5), 5.38-5.13 ppm (f, -$C_6H_5CH_2$), 4.74-4.5 ppm (h, g, -CH) and 2.91 ppm (o, n, -CH) indicated the successful synthesis of PLL(Z)-*b*-PPhe (Fig. 1B). Through the integral analysis, the ratio of PLL(Z) to PPhe was 3:6, 3:3.6, 3:2, respectively, which basically showed PPhe with different rations had been grafting on PLL(Z) to form three types of PLL(Z)-*b*-PPhe successfully. Following with GPC characterization (Fig. S1 in Supporting information), we found the curves of the three types of PLL-*b*-PPhe copolymer all showed only one peak, indicated only one polymer in the final products. And the molecular weight of PLL-*b*-PPhe calculated by GPC listed in Table S1 (Supporting information), which was close to the designed molecular weight.

The transfection performance of PLL-*b*-PPhe was mainly evaluated by a siRNA silencing *in vitro*. The HeLa-luc cells that persistently express of luciferase were used for transfection with selected gene Bcl2 siRNA and the non-acting gene NC siRNA. The transfection performance of the materials was evaluated by the difference between the silencing efficiency of Bcl2 siRNA and NC siRNA. Fig. 2 showed the results of transfection with different

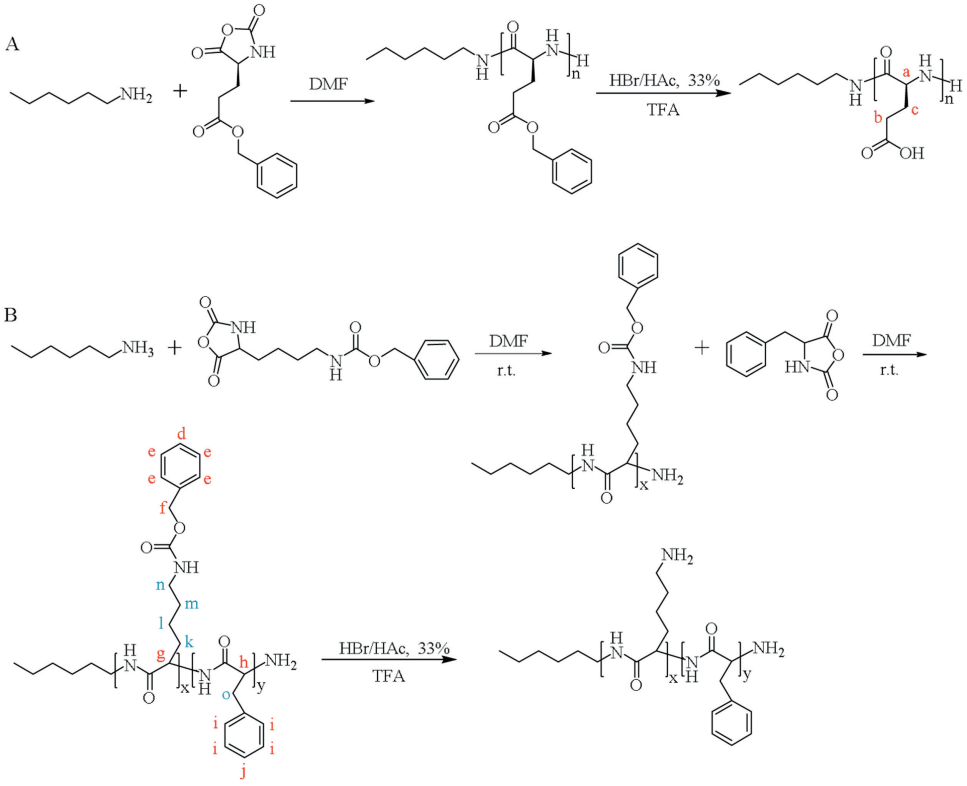

Scheme 2. The synthesis of (A) the PG and (B) the diblock copolymer PLL-*b*-PPhe.

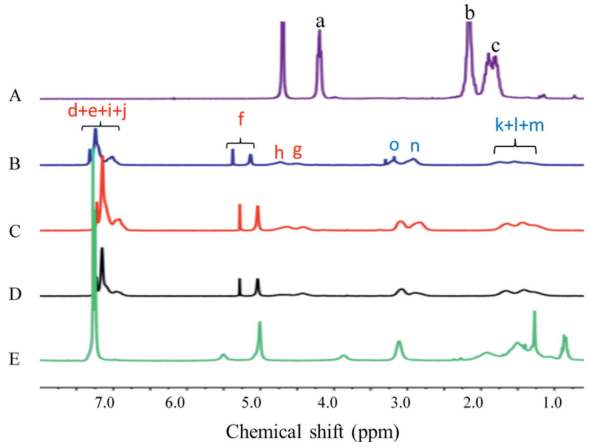

Fig. 1. ^{1}H NMR spectra of (A) PG, (B) PLL:PPhe (30:60), (C) PLL:PPhe (30:40), (D) PLL:PPhe (30:20), (E) PLL(Z).

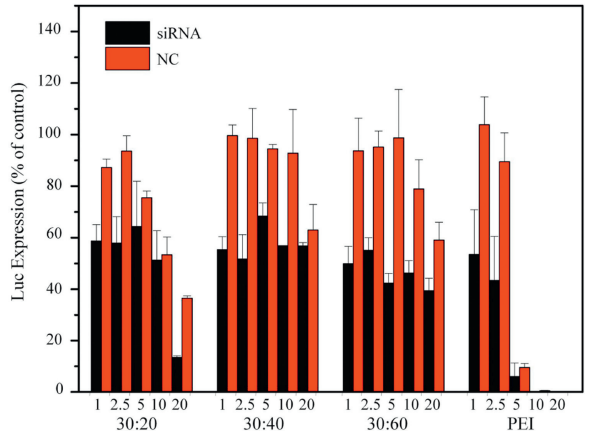

Fig. 2. Transfection effect of different molar of PLL-*b*-PPhe. The PLL-*b*-PPhe/siRNA with different mass ratios (2.5:1, 5:1, 10:1, and 20:1) and PLL/PPhe molar ratios are 30:20, 30:40, 30:60 and PEI25k, respectively.

molar ratios of PLL-*b*-PPhe at 24 h, in which the low expression of luciferase proved that the material had a high silencing effect. And the high silencing efficiency of materials by NC siRNA indicated that the material was highly toxic. The result indicated PLL-*b*-PPhe/Bcl2 siRNA had the similar silencing effect on the express of luciferase as PEI, especially in PLL-*b*-PPhe with a molar ratio of 30:60. When the mass ratio of PLL-*b*-PPhe to Bcl2 siRNA was 5:1, it had the best silencing effect.

To characterize the ability of PLL-*b*-PPhe self-assembling into micelles in aqueous solution, the critical micelle concentration (CMC) was tested and shown in Fig. 3A as 0.0396 mg/mL. So the micelles can be stable as long as the material concentration was higher than 0.0396 mg/mL. Then the micelles were used to carry DOX as PLL-*b*-PPhe/DOX. The particle sizes of PLL-*b*-PPhe micelles and PLL-*b*-PPhe/DOX detected by DLS were around 98.4 nm and 49.8 nm, respectively (Fig. 3B). Interestingly, after the drug was loading, the particle size became smaller due to hydrophobic interaction between the PLL-*b*-PPhe and DOX, which was also observed by TEM (Fig. 3C). And the morphologies of PLL-*b*-PPhe before and after drug loading were both spheres. The particle sizes of PLL-*b*-PPhe/DOX/Bcl2 siRNA were 54 nm, which was closed to PLL-*b*-PPhe/DOX (Fig. S2 Supporting information). Moreover, the drug loading was 7.98%, and the encapsulation efficiency was 36.7%.

The DOX released from PG/PLL-*b*-PPhe/DOX was tested and shown in Fig. 4. The cumulative drug release increased with the

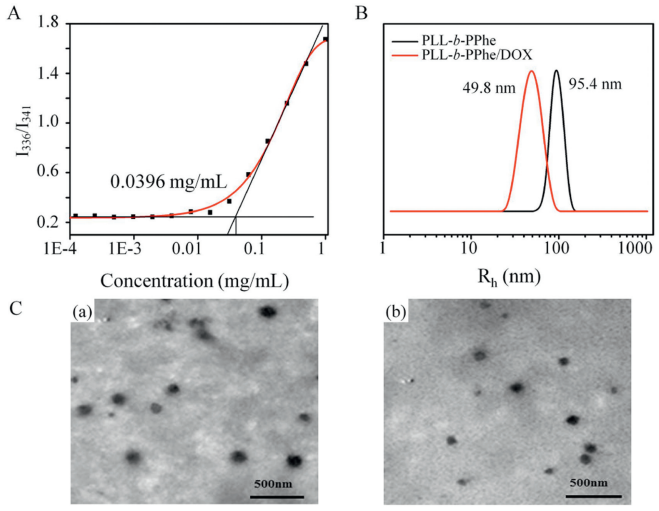

Fig. 3. (A) The critical micelle concentration (CMC) of PLL-*b*-PPhe. (B) The hydrodynamic radii (R_h) of PLL-*b*-PPhe and PLL-*b*-PPhe/DOX. (C) The TEM images of (a) PLL-*b*-PPhe (b) PLL-*b*-PPhe/DOX.

decreasing pH, and reached to 60% for 24 h at pH 6.8, slightly below that at pH 5.0. This result demonstrated that the codelivery system was pH sensitive, which caused more drug release in acidic tumor microenvironment, and the system was suitable for cancer therapy. When co-carried with siRNA, PG/PLL-*b*-PPhe/DOX/Bcl2 siRNA was also pH sensitive (Fig. S3 in Supporting information).

The zeta potential of PLL-*b*-PPhe and PG/PLL-*b*-PPhe were shown in Fig. 5A. PLL-*b*-PPhe had a positive charge of 31 mV. The addition of PG significantly reduced the potential to 12 mV. The complexes of PG/PLL-*b*-PPhe were added into B16F10 cells to demonstrate that PG shielding could reduce cytotoxicity (Fig. S4 in Supporting information). From MTT test, PG reduced the cytotoxicity of PLL-*b*-PPhe micelles.

The cytotoxicity of the co-delivery system against B16F10 cells was investigated and showed in Fig. 5B. The viability of B16F10 cells decreased with DOX concentration increasing, and PG/PLL-*b*-PPhe/DOX/Bcl2 siRNA was more cytotoxic than PG/PLL-*b*-PPhe/DOX and others. When the DOX concentration was increased to 1 μg/mL, the viability of B16F10 cells treated with PG/PLL-*b*-PPhe/DOX/Bcl2 siRNA and PG/PLL-*b*-PPhe/DOX/NC siRNA had the most significant differences, indicated Bcl2 siRNA started to take effects.

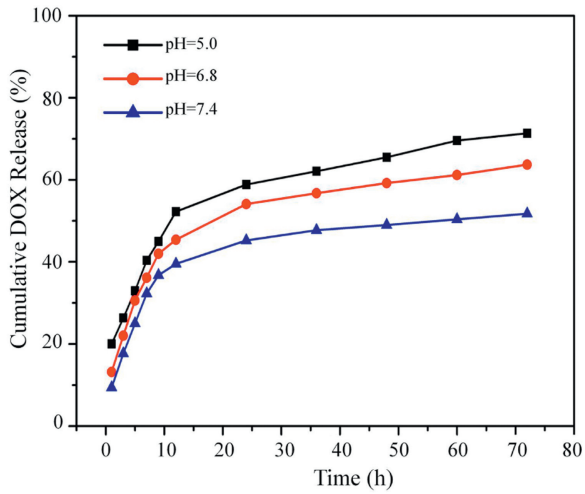

Fig. 4. Drug release of PG/PLL-*b*-PPhe/DOX at different pH.

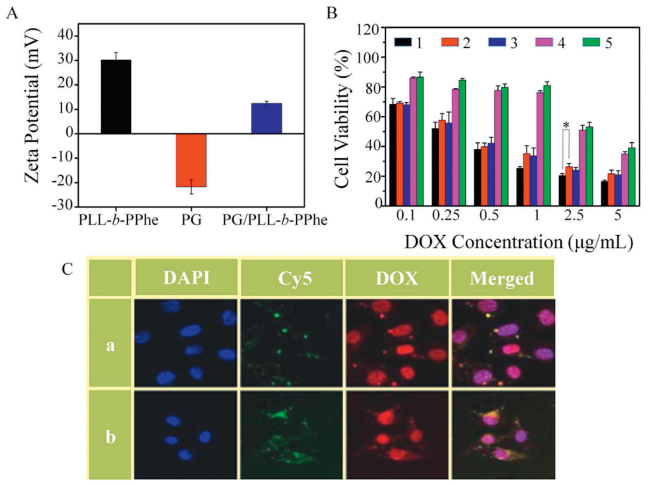

Fig. 5. (A) Zeta potential of PLL-*b*-PPhe, PG and PG/PLL-*b*-PPhe. (B) Synergistic therapeutic effect of PG/PLL-*b*-PPhe/DOX/Bcl2 siRNA (1: PG/PLL-*b*-PPhe/DOX/Bcl2 siRNA, 2: PG/PLL-*b*-PPhe/DOX/NC siRNA, 3: PG/PLL-*b*-PPhe/DOX, 4: PG/PLL-*b*-PPhe/Bcl2 siRNA, 5: PG/PLL-*b*-PPhe/NC siRNA, $^{*}P < 0.05$). (C) Cell uptake of PG/PLL-*b*-PPhe/DOX/Cy5 siRNA (a: 3 h, b: 24 h).

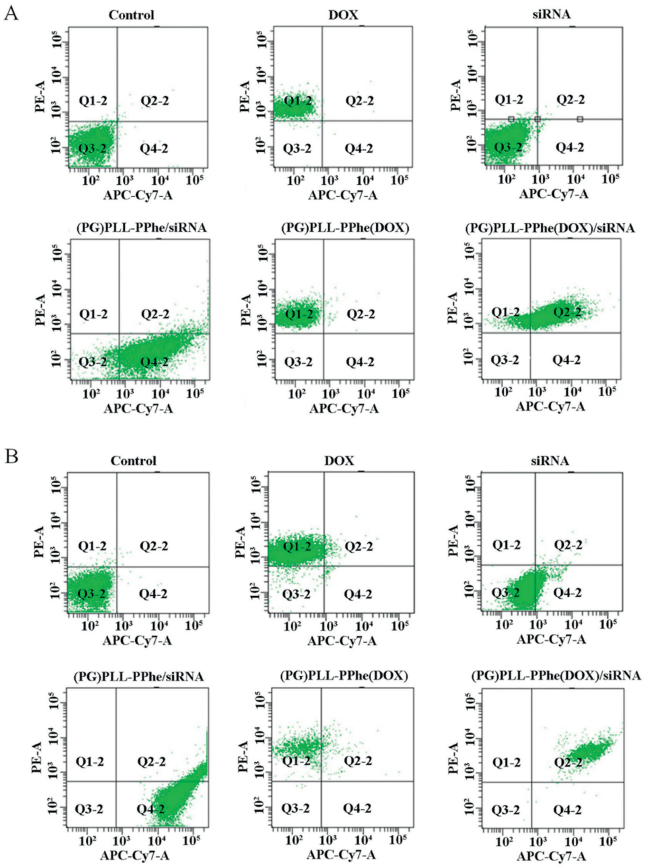

Fig. 6. Intracellular distribution of PG/PLL-*b*-PPhe/DOX/Cy5 siRNA carrying drugs and genes at (A) 3 h, (B): 24 h.

So the PG/PLL-*b*-PPhe/DOX/Bcl2 siRNA co-delivery system had the best killing effect on B16F10 cells.

Fig. 5C showed the distribution of genes and drugs from PG/PLL-*b*-PPhe/DOX/Cy5 siRNA in B16F10 cells cultured at 3 h and 24 h. The fluorescence intensity of the DOX can be clearly observed in the nuclear region at 3 h and 24 h, and the fluorescence of DOX was more pronounced at 24 h than at 3 h. In addition, the green fluorescence on the photograph was from Cy5 siRNA. At 3 h, Cy5 siRNA had been delivered into the cells, and at 24 h, the fluorescence signal of Cy5 siRNA was more evenly distributed around the nucleus than 3 h. This demonstrated that the PG/PLL-*b*-PPhe/DOX/Cy5 siRNA co-delivery system had more efficiently endocytosed by B16F10 cells.

The cell uptake of PG/PLL-*b*-PPhe/DOX/Cy5 siRNA was also studied by flow cytometry at 3 h and 24 h and shown in Fig. 6, where the ordinate was the fluorescence of DOX and the abscissa was the fluorescence emitted by the Cy5 siRNA. It was not difficult to find that the fluorescence absorption of PLL-*b*-PPhe/Cy5 siRNA was stronger than Cy5 siRNA alone, while PLL-*b*-PPhe/DOX also had stronger absorption than DOX. PLL-*b*-PPhe/DOX/Cy5 siRNA codelivery system had both higher gene and DOX endocytosis. Therefore, the co-delivery system was more efficient in delivering both genes and drugs into B16F10 cells simultaneously.

In this paper, different mass ratio (30:20, 30:40, 30:60) of the amphiphilic diblock copolymer PLL-*b*-PPhe were designed and synthesized successfully, and their structures were analyzed by ^{1}H NMR and GPC. For PLL-*b*-PPhe was amphiphilic, it can self-assemble into micelles in aqueous solution. The PLL-*b*-PPhe micelles were stable demonstrated by CMC, DLS, and TEM. The CMC was 0.0396 mg/mL. DLS and TEM indicated that the particle size of the micelles decreased after drug loading due to hydrophobic interaction. The cumulative drug release increased with the pH decreasing, and reached to 60% for 24 h at pH 6.8, slightly below that at pH 5.0, confirmed the system was pH sensitive. PG was synthesized to shield positive charge of the PLL-*b*-PPhe micelles to reduce cytotoxicity and the zeta potential of PLL-*b*-PPhe was reduced from 30 mV to 12 mV after shielding. Then, Bcl2 siRNA and DOX co-carried in PG/PLL-*b*-PPhe to form PG/PLL-*b*-PPhe/DOX/ Bcl2 siRNA co-delivered system, which had obvious synergistic therapeutic effects of drug and gene. Finally, PG/PLL-*b*-PPhe/DOX/Bcl2 siRNA endocytosed by B16F10 cells was characterized by CLSM and flow cytometry, indicated the co-delivery system can be endocytosed by B16F10 cells efficiently. As a result, the co-delivery system can deliver genes and drugs into B16F10 cells together and perform effective synergistic cancer therapy.

Declaration of competing interest

The authors declare that they have no known competing financial interests or personal relationships that could have appeared to influence the work reported in this paper.

Acknowledgments

The authors are thankful to the National Natural Science Foundation of China (No. 51873208), the National Science and Technology Major Projects for Major New Drugs Innovation and Development (No. 2018ZX09711003-012), National Program for Support of Top-notch Young Professionals, Jilin Province Science and Technology Development Program (No. 20180414027GH) for financial support to this work.

Appendix A. Supplementary data

Supplementary material related to this article can be found, in the online version, at doi:https://doi.org/10.1016/j.cclet.2020.02.034.

References

[1] F. Bray, J. Ferlay, I. Soerjomataram, et al., CA-Cancer J. Clin. 68 (2018) 394–424.
[2] H. Fang, Z. Guo, L. Lin, et al., J. Am. Chem. Soc. 140 (2018) 11992–12000.

[3] J. Liu, H.J. Li, Y.L. Luo, et al., ACS Nano 13 (2019) 8648–8658.
[4] H.F. Wang, R. Ran, Y. Liu, et al., ACS Nano 12 (2018) 11600–11609.
[5] C. Yao, J. Tian, H. Wang, et al., Chin. Chem. Lett. 28 (2017) 893–899.
[6] J. Ding, J. Chen, L. Gao, et al., Nano Today 29 (2019) 100800.
[7] V. Torchilin, Adv. Drug. Deliver. Rev. 63 (2011) 131–135.
[8] L. Yan, S.H. Crayton, J.P. Thawani, et al., Small 11 (2015) 4870–4874.
[9] H. Zheng, Y. Zhang, L. Liu, et al., J. Am. Chem. Soc. 138 (2016) 962–968.
[10] H. Meng, M. Wang, H. Liu, et al., ACS Nano 9 (2015) 3540–3557.
[11] D. Hanahan, R.A. Weinberg, Cell 144 (2011) 646–674.
[12] F.J. Sharom, J. Membrane Biol. 160 (1997) 161–175.
[13] X. Guan, Y. Li, Z. Jiao, et al., ACS Appl. Mater. Interfaces 7 (2015) 3207–3215.
[14] K. Han, Q. Lei, H.Z. Jia, et al., Adv. Funct. Mater. 25 (2015) 1248–1257.
[15] H. Tian, Z. Guo, L. Lin, et al., J. Control. Release 174 (2014) 117–125.
[16] C.H. Ahn, S.Y. Chae, Y.H. Bae, S.W. Kim, J. Control. Release 80 (2001) 273–282.
[17] J. Lina, Y. Zou, C. Wang, et al., Mater. Sci. Eng. C 44 (2014) 430–439.
[18] Q. Zhu, Y. Zhou, M. Guan, et al., Biomaterials 35 (2014) 5965–5976.
[19] A.H. Dantzig, R.L. Shepard, J. Cao, et al., Cancer Res. 56 (1996) 4171–4179.
[20] D. Decaudin, S. Geley, T. Hirsch, et al., Cancer Res. 57 (1997) 62–67.
[21] R.T. Lima, L.M. Martins, J.E. Guimaraes, C. Sambade, M.H. Vasconcelos, Cancer Gene Ther. 11 (2004) 309–316.
[22] C.N. Xu, H.Y. Tian, Y.B. Wang, et al., Chin. Chem. Lett. 28 (2017) 807–812.
[23] F.M. Wensveen, N.L. Alves, I.A. Derks, K.A. Reedquist, E. Eldering, Apoptosis 16 (2011) 708–721.
[24] J.E. Chipuk, T. Moldoveanu, F. Llambi, M.J. Parsons, D.R. Green, Mol. Cell 37 (2010) 299–310.
[25] M.L. Patil, M. Zhang, T. Minko, ACS Nano 5 (2001) 1877–1887.
[26] G.G. McGill, M. Horstmann, H.R. Widlund, et al., Cell 109 (2002) 707–718.
[27] H. Tian, L. Lin, Z. Jiao, et al., J. Control. Release 172 (2013) 410–418.
[28] C. Zheng, M. Zheng, P. Gong, et al., Biomaterials 34 (2013) 3431–3438.
[29] Z. Luo, P. Li, J. Deng, et al., J. Control. Release 170 (2013) 259–267.
[30] J. Deng, N. Gao, Y. Wang, et al., Biomacromolecules 13 (2012) 3795–3804.
[31] T. Kurosaki, T. Kitahara, S. Kawakami, et al., J. Control. Release 142 (2010) 404–410.
[32] J. Chluba, J.C. Voegel, G. Decher, et al., Biomacromolecules 2 (2001) 800–805.